

SCHEDDING LIGHT ON CARBON-OXYGEN WHITE DWARF MERGERS AND POST-MERGER  
EVOLUTION

by

Chenchong Zhu

A thesis submitted in conformity with the requirements  
for the degree of Doctor of Philosophy  
Graduate Department of Astronomy & Astrophysics  
University of Toronto

© Copyright 2016 by Chenchong Zhu

## **Abstract**

Shedding Light on Carbon-Oxygen White Dwarf Mergers and Post-Merger Evolution

Chenchong Zhu

Doctor of Philosophy

Graduate Department of Astronomy & Astrophysics

University of Toronto

2016

“Do or do not; there is no try.”

*–Yoda*

## **Acknowledgements**

I'd like to thank the academy for choosing me...

# Contents

<b>1</b>	<b>Introduction</b>	<b>1</b>
1.1	White Dwarf Mergers . . . . .	1
1.1.1	The Panopoly of Stellar Mergers . . . . .	1
1.1.2	Mergers of WD Binaries . . . . .	1
1.2	The Mystery of Type Ia Supernovae . . . . .	2
1.2.1	Properties and Traditional Formation Channels of SNe Ia . . . . .	2
1.2.2	Traditional Shortfalls . . . . .	2
1.2.3	Brave New Channels . . . . .	2
1.3	The vK10 SN Ia Channel . . . . .	2
1.3.1	Channel Overview and Advantages . . . . .	2
1.3.2	But Will it Blend? (Thesis Motivation) . . . . .	2
1.4	Physics of the WD Merging Process . . . . .	2
1.4.1	Stable and Unstable Mass Transfer . . . . .	2
1.4.2	Are Merging WDs Co-Rotating? . . . . .	2
1.5	Post-Merger Evolution . . . . .	2
1.6	Thesis Overview . . . . .	2
<b>2</b>	<b>A Parameter-Space Study of Carbon-Oxygen White Dwarf Mergers</b>	<b>3</b>
2.1	Introduction . . . . .	4
2.2	Code and Input Physics . . . . .	5
2.2.1	The SPH Code . . . . .	6
2.2.2	Initial Conditions . . . . .	7
2.2.3	Merger Completion Time . . . . .	8
2.3	Results . . . . .	9
2.3.1	Representative Mergers . . . . .	9
	<b>Bibliography</b>	<b>12</b>

# **List of Tables**

# List of Figures

- 2.1 Structure of a  $0.4 - 0.8 M_{\odot}$  merger remnant, representing the general outcome of a merger of white dwarfs with dissimilar mass. Upper left and middle – binned maps of density  $\rho$  and temperature  $T$  along slices in the  $xy$  and  $xz$ -planes. Lower left – binned maps and contours of density, temperature, and angular frequency  $\Omega$  in the  $(\omega, z)$  plane, averaged over cylindrical coordinate  $\phi$  and over  $\pm z$  (with 1 added to  $\Omega$  to avoid problems with the logarithmic intensity scale). Middle – enclosed masses of donor and accretor material  $M_d$  and  $M_a$  (solid red and blue, resp.), and fraction of donor material  $f_d$  at a particular mass shell (dashed magenta). Middle, one but lowest – temperature-density profile with enclosed masses in  $0.2 M_{\odot}$  increments indicated, both along the equatorial plane (solid curve, squares) and along the rotational axis (dot-dashed curve, circles). Middle, bottom – enclosed mass as a function of  $r$ , with the total mass indicated by the horizontal dashed red line. Right-hand column, top to bottom – density, temperature, entropy, angular (cyan) and Keplerian (blue) frequency, and degeneracy (blue), thermal (red) and rotational (cyan) specific energies as a function of enclosed mass  $M$ , both along the equatorial plane and along the rotational axis (solid and dot-dashed curves, respectively). In all graphs, the start of the disk (where the centrifugal acceleration equals half the gravitational one) and the equatorial radius (or mass enclosed within) of maximum temperature are marked by vertical green and blue dashed lines, respectively. [See the electronic edition of the Journal for Figs. 1.1–1.48.] . . . . . 10
- 2.2 As Fig. Set 2.1, but for a  $0.6 - 0.6 M_{\odot}$  merger remnant, representing the general outcome of a similar-mass merger. . . . . 11

# Chapter 1

## Introduction

### 1.1 White Dwarf Mergers

#### 1.1.1 The Panopoly of Stellar Mergers

Approximately two out of every three stars are born into a binary system. A substantial fraction of these stars will interact, some due to their orbital separation at birth, while others following the expansion of one or both constituent stars as they evolve off of the main sequence. These interactions primarily take form as mass transfer between the stars (Yungelson 2005), and if mass transfer becomes unstable (increases exponentially over time), it ends with the violent coalescence of the two stars into one. These stellar mergers, like other forms of binary interaction, disrupt single star evolution and create merged products, or “merger remnants”, with unusual properties including blue stragglers (eg. Andronov et al. 2006; Knigge et al. 2009), luminous blue variables (Justham et al. 2014), subdwarf OB and R Corona Borealis stars. They also liberate tremendous amounts of energy and eject significant amounts of mass, giving rise to a cornucopia of electromagnetic and gravitational-wave transients ranging from luminous red novae (from the merger of two (post-) main-sequence stars; eg. V838 Monocerotis and V1309 Scorpii (Tylenda et al. 2011; Nandez et al. 2014)) to short gamma-ray bursts (from two neutron stars; eg. Rosswog (2015)) and the gravitational wave outburst from coalescing stellar-mass black holes (as recently found by the LIGO detector; Abbott et al. 2016). Indeed, with current deep and short-cadence optical/near-infrared survey projects such as the Palomar Transient Factory (Rau et al. 2009) and Pan-STARRS (Kaiser et al. 2010) continuing to uncover more rare and even hitherto-unknown transients, and the ambitious Large Synoptic Survey Telescope (LSST Science Collaboration et al. 2009) under construction, a much more complete picture of merger-generated transients will form over the next decade.

#### 1.1.2 Mergers of WD Binaries

One common end-product of binary stellar evolution is the merger of two white dwarfs (WDs) in a close binary orbit. Close WD binaries are formed as a result of at least two phases of mass transfer (at least one of which is a common envelope event) during the binary’s prior stellar evolution. These mass transfer phases act to sap the orbital angular momentum of the

## **1.2 The Mystery of Type Ia Supernovae**

### **1.2.1 Properties and Traditional Formation Channels of SNe Ia**

#### **1.2.2 Traditional Shortfalls**

#### **1.2.3 Brave New Channels**

## **1.3 The vK10 SN Ia Channel**

### **1.3.1 Channel Overview and Advantages**

### **1.3.2 But Will it Blend? (Thesis Motivation)**

## **1.4 Physics of the WD Merging Process**

### **1.4.1 Stable and Unstable Mass Transfer**

### **1.4.2 Are Merging WDs Co-Rotating?**

## **1.5 Post-Merger Evolution**

## **1.6 Thesis Overview**

## Chapter 2

# A Parameter-Space Study of Carbon-Oxygen White Dwarf Mergers

Chenchong Zhu, Philip Chang, Marten H. van Kerkwijk and James Wadsley  
The Astrophysical Journal **some crap**

As we discussed in Sec. ??, the merger of two carbon-oxygen white dwarfs can lead either to a spectacular transient, stable nuclear burning or a massive, rapidly rotating white dwarf. Previous simulations of mergers have shown that the outcome strongly depends on whether the white dwarfs are similar or dissimilar in mass (?). In the similar-mass case, both white dwarfs merge fully and the remnant is hot throughout, while in the dissimilar case, the more massive, denser white dwarf remains cold and essentially intact, with the disrupted lower mass one wrapped around it in a hot envelope and disk.

In order to determine what constitutes “similar in mass” and more generally how the properties of the merger remnant depend on the input masses, we simulated unsynchronized carbon-oxygen white dwarf mergers for a large range of masses using smoothed-particle hydrodynamics. We find that the structure of the merger remnant varies smoothly as a function of the ratio of the central densities of the two white dwarfs. A density ratio of 0.6 approximately separates similar and dissimilar mass mergers. Confirming previous work, we find that the temperatures of most merger remnants are not high enough to immediately ignite carbon fusion. During subsequent viscous evolution, however, the interior will likely be compressed and heated as the disk accretes and the remnant spins down. We find from simple estimates that this evolution can lead to ignition for many remnants. For similar-mass mergers, this would likely occur under sufficiently degenerate conditions that a thermonuclear runaway would ensue.

## 2.1 Introduction

A few percent of all white dwarfs (WDs) will eventually merge with another white dwarf. The outcome of such mergers will depend on the compositions of the WDs involved. For two helium WDs, a low-mass helium star might result, which would be observed as an sdOB star. For a helium WD merging with a carbon-oxygen one, a helium giant could form, observable as a hydrogen-deficient giant or R CrB star. For two carbon-oxygen WDs (CO WDs), the outcome could vary between simply a more massive WD, a carbon-burning star, an explosion, or collapse to a neutron star, depending on whether stable or unstable carbon fusion is ignited, and whether the total mass exceeds the critical mass for pycnonuclear ignition or electron captures (both close to the Chandrasekhar mass  $M_{\text{Ch}}$ ). For mergers involving an oxygen-neon WD, the mass will always be high, and explosive demise or transmutation seems inevitable.

The outcome of the merger of two CO WDs is uncertain in part because during the merger temperatures do not become hot enough to ignite significant carbon fusion (e.g., ?, ? hereafter), except possibly for masses above  $\sim 0.9 M_{\odot}$  (??). Hence, the final fate depends on subsequent evolution, in which differential rotation is dissipated, the remnant disk accretes, and the whole remnant possibly spins down. Due to these processes, the remnant could be compressed and heated, which, if it happens faster than the thermal timescale, would lead to increased temperatures and thus potentially to ignition.

So far, efforts have focused on merging binaries with total mass  $M > M_{\text{Ch}}$ . The end result of such mergers is believed to be either stable off-center carbon ignition, which would turn the merger remnant into an oxygen-neon WD and possibly eventually result in accretion-induced collapse (?), or slow accretion, which allows the remnant to stay cool and eventually ignite at high central density (?). Less massive mergers were usually thought to result in more massive, rapidly rotating CO WDs (??), but more recently it has been realized these might eventually become hot enough to ignite (van Kerkwijk et al. 2010, vK10 hereafter; ??). Indeed, vK10 argue that type Ia supernovae result generally from mergers of CO WDs with similar masses, independent of whether or not their total mass exceeds  $M_{\text{Ch}}$  (see below). For all these studies, the conclusions on whether and where ignition takes place depend critically on the structure of the merger remnant.

The merging process, and the merger remnant, have been studied quite extensively, mostly using smoothed-particle hydrodynamics (SPH; e.g. ?). These simulations have shown that the outcome strongly depends on whether the WDs are similar or dissimilar in mass. In the similar-mass case, both WDs disrupt fully and the remnant is hot throughout, while in the dissimilar case, the more massive, denser WD remains essentially intact and relatively cold, with the disrupted lower mass one wrapped around it in a hot envelope and disk. Less clear, however, is what constitutes “similar-mass,” and, more generally, how the merger remnant properties depend on the initial conditions.

In principle, for cold WDs of given composition, the remnant properties should depend mostly on the two WD masses, with a second-order effect due to rotation. In this paper, we try to determine these dependencies using simulations of WD mergers with the Gasoline SPH code, covering the entire range of possible donor and accretor masses, but limiting ourselves to non-rotating WDs. Our primary aim is to identify trends between mergers of different masses, both to guide analytical understanding and to help scale other, perhaps more precise simulations. Here, our hope is that while the results of individual simulations may suffer from uncertainties related to the precise techniques and assumptions used, the trends should be more robust. We also try to provide sufficient quantitative detail on the

properties of merger remnants that it becomes possible to make analytical estimates or construct reasonable numerical approximations without having to run new simulations.

Our work is complementary to the recent surveys of remnant properties by ? and ?, in that they focus on different scientific questions (e.g., orbital stability; possible detonation). In contrast to our work, they assume that the WDs are co-rotating with the orbit. Whether this is a better assumption than no rotation depends on the strength of tidal dissipation, which unfortunately is not yet known (see ??).

Our work also is part of a series of numerical studies investigating the viability of sub-Chandrasekhar mass (sub- $M_{\text{Ch}}$ ) CO WD mergers producing SNe Ia, as proposed by vK10. This channel relies on similar-mass mergers producing remnants that are hottest near the center, and on compressional heating by subsequent accretion and/or magnetically mediated spin-down leading to ignition. The advantages of this channel are that it accounts for the absence of direct evidence for stellar companions, the observed SN Ia rate, and the dependence of SN Ia peak luminosity on the age of the host stellar population (because lower-mass merger constituents take longer to form). Since pure detonations of sub- $M_{\text{Ch}}$  CO WDs produce light curves very similar to observed SNe Ia (??), it also removes the need for imposed deflagration-to-detonation transitions. Important questions, however, remain, including what fraction of mergers leads to remnants that are hot near the center (in highly degenerate conditions), how the subsequent viscous phase proceeds in detail, whether ignition leads to a detonation, and whether the detonation of a remnant that may still rotate and be surrounded by a disk would produce an event similar to an SN Ia. With our work, we attempt to address the first question.

This paper is organised as follows. In Section 2.2, we describe the SPH code we used, as well as our initial conditions. In Section 2.3, we present our results and give trends for a number of pertinent remnant properties. In Section ??, we test the robustness of our results, and in Section ?? compare our results with those of ? and others. Lastly, in Section ??, we speculate on the further evolution of our remnants, considering in particular whether, as suggested by vK10, some might lead to type Ia supernovae.

## 2.2 Code and Input Physics

We simulate the mergers by placing non-rotating white dwarfs in a circular orbit with an initial separation  $a_0$  chosen such that rapid mass transfer begins immediately. We then follow the merger for six orbits, at which time the remnant has become approximately axisymmetric. As in prior work, the morphology of all merger remnants is similar, consisting of a dense, primarily degeneracy-supported center surrounded by a partly thermally-supported hot envelope (called a “corona” by ?) and a thick, sub-Keplerian disk. We will use the terms “core”, “envelope” and “disk” throughout this work. We also quite often refer to both the core and envelope simultaneously as the “core-envelope”.

We use simulation techniques and initial conditions that are standard in the field of WD merger simulations, both in order to compare with previous work, as well as to not introduce novel numerical effects into our simulations. We detail our code and initial conditions below so that they can easily be reproduced.

### 2.2.1 The SPH Code

With smoothed-particle hydrodynamics, one uses particles as a set of interpolation points to determine continuum values of the fluid and model its dynamics. SPH is a Lagrangian method, meaning movement is automatically tracked, and regions of high density contain more particles and therefore are automatically more resolved. Moreover, SPH inherently conserves angular momentum in three dimensions, which is difficult to reproduce in grid codes except under specific coordinate systems and symmetries. SPH therefore allows one to efficiently simulate complex phenomena with a large range of lengthscales. It has become the method of choice for merger simulations, and so we chose it as well.

For our simulations, we use Gasoline (?), a modular tree-based SPH code that was designed and has been used for a wide range of astrophysical scenarios, from galaxy interactions to planet formation. It aims for tight controls on force accuracy and integration errors. Gasoline implements the ? kernel – we use 100 neighbors – and uses the asymmetric energy formulation (?; Eqn. 8) to evolve particle internal energy. In our simulations, total energy is on average conserved to 0.3%, and angular momentum to 0.006%.

By default, Gasoline uses the usual Monaghan and Gingold formulation for artificial viscosity (see ?), together with a Balsara switch (a standard feature of WD merger SPH simulations) to reduce viscosity in non-shocking, shearing flows. ? found that such a prescription did not reduce viscosity sufficiently, resulting in excess spin-up of the remnant core and associated shear heating. ?, in addition to a Balsara switch, used variable coefficients for the linear and quadratic viscosity terms in the SPH equations of motion and energy, setting these values to  $\alpha = 0.05$  and  $\beta = 0.1$ , respectively, where shocks are absent, and around unity where they are present. A similar formulation was used in ???. Since Gasoline includes it as well, we have used it for our study. Excess viscosity nevertheless remains a potential problem; we investigate its effects further in Sec. ??.

We modified Gasoline to include support for degenerate gas through the Helmholtz equation of state (EOS)<sup>1</sup> (?). This code, also used in ? and ?'s simulations, interpolates the Helmholtz free energy of the electron-positron plasma, along with analytical expressions for ions and photons, to determine pressure, energy and other properties from density and temperature. It is fast, spans a large range of density and temperature, and has, by construction, perfect thermodynamic consistency. To obtain quantities as a function of density and internal energy, we utilized a Newton-Raphson inverter. To keep the energy-temperature relation positive-definite, we did not disable Coulomb corrections in cases where total entropy became negative.

Gasoline keeps track of the internal energy of particles, using it to determine other thermodynamic properties for fluid evolution. A particle's energy will naturally fluctuate due to noise, but for nearly zero-temperature particles this could result in their energy dipping below the Fermi energy. In such situations we keep the pressure at the Fermi pressure, while letting the energy freely evolve. A consequence of the floor is that a small amount of excess energy is injected into the system through mechanical work, which eventually manifests as additional thermal energy. The accumulated energy over a simulation is typically a small fraction of the internal energy, and therefore does not significantly affect the dynamics of the merger or most properties of the remnant. In cold, degeneracy-dominated material, however, a small change in internal energy corresponds to a large temperature change, at times comparable to the physically expected values, and thus the temperatures near the centers of some of our simulations have been affected. We characterize this spurious heating in Sec. ?? and show

---

<sup>1</sup> Available at <http://cococubed.asu.edu/>.

that it does not unduly affect our work’s conclusions. However, it makes it difficult to run much longer simulations.

We also place an energy floor at half the Fermi energy. This is to prevent particle energies from approaching zero (and consequently calling for tiny timesteps), which under rare circumstances occurs when particles perform a great deal of mechanical work. We find this happens primarily for particles that are flung out of the system by the merger and are cooling rapidly, and therefore are confident it has only a very minor effect on our simulations.

In our work, we ignore outer hydrogen and helium layers, composition gradients, and any nuclear reactions. This is mainly because previous work has found that nuclear processing was unimportant during the merger. For instance, ? found fusion released  $\sim 10^{41}$  erg for their  $0.6 - 0.8 M_{\odot}$  merger, orders of magnitude smaller than the  $\sim 10^{50}$  erg binding energy of the remnant. Only for mergers involving very massive,  $\gtrsim 0.9 M_{\odot}$  WDs might this assumption break down, with the possibility of carbon detonations arising (??; but see ??). Similarly, ?, who included standard helium envelopes of  $\sim 1 - 2\%$  of the WD mass in their simulations, found that only for accretors with masses above  $\sim 1 M_{\odot}$  did it make a substantial difference: a helium detonation would inject  $\sim 10^{49}$  erg into the merger remnant. While this led to additional heating, it was insufficient to trigger much carbon burning or unbind any portion of the remnant (helium detonations have also been found for lower-mass accretors with CO-He hybrid donors; ?).

### 2.2.2 Initial Conditions

We created spherical white dwarfs using pre-relaxed cells of particles rescaled to follow the appropriate enclosed mass-radius relation determined using the Helmholtz equation of state. We assumed a composition of 50% carbon and 50% oxygen by mass, and a uniform temperature of  $5 \times 10^6$  K. The stars were then relaxed in Gasoline for 81 s ( $\sim 10 - 40$  dynamical times, depending on the white dwarf mass) with thermal energy and motion damped (to  $5 \times 10^6$  K and  $0 \text{ cm s}^{-1}$ , respectively) during the first 41 s, and left free during the remaining 40 s. Particle energy noise prevented cooling of  $\gtrsim 5 \times 10^6 \text{ g cm}^{-3}$  material to below  $10^7$  K. We checked that the density profile of each star after relaxation was consistent with the solution from hydrostatic equilibrium, and found this was the case – central densities, for example, agreed to within 2%. The radii of the relaxed stars, as defined by the outermost particle of a relaxed WD, on the other hand were on average about 7% too small, reflecting our inability to model the tenuous WD outer layers<sup>2</sup>.

We used a constant particle mass of  $10^{28}$  g, so that a  $0.4 M_{\odot}$  WD has  $8 \times 10^4$  particles, and a  $1.0 M_{\odot}$  WD has  $2 \times 10^5$ . These numbers are similar to those used by ? and ?, and exceed the  $\sim 2 \times 10^4$  particles per star used by ?. ? performed a resolution test for a merger of two  $0.81 M_{\odot}$  WDs, varying the number of particles per star from  $10^5$  to  $2 \times 10^6$ . They found differences of  $\sim 2\%$  in the mass of the core plus envelope, disk half-mass radius, and inner disk rotation frequency. The one qualitative difference they found was that at their highest particle resolution, the WDs failed to break symmetry and disrupt (note that they assumed co-rotating WDs, making such a stable contact configuration possible). We perform our own test in Sec. ?? and find similar results.

We relaxed  $0.4, 0.5, 0.55, 0.6, 0.65, 0.7, 0.8, 0.9$  and  $1.0 M_{\odot}$  white dwarfs, and combined them in all

---

<sup>2</sup>Our relaxed WDs also show evidence of sub-kernel radial banding of particles, which does not appear in any interpolated quantities. We do not believe this banding has an effect on our simulations except for a possible reduction in effective resolution, but will investigate remedies in future work.

possible permutations to form our parameter space of binaries. These values were chosen to represent the range of possible CO WD masses, with greater resolution near the empirical peak at  $\sim 0.65 M_{\odot}$  of the mass distribution of (single) CO WDs (?). We also performed additional simulations with  $0.575 - 0.65$ ,  $0.625 - 0.65$  and  $0.64 - 0.65 M_{\odot}$  binaries to explore the outcomes of similar-mass mergers. We thus simulated 48 mergers in total.

We placed two relaxed, irrotational WDs in a circular orbit. We chose the initial separation  $a_0$  such that the donor WD just fills its Roche lobe, taking the location of the donor’s outermost particle as its radius and using the Roche lobe approximation (for a synchronized binary) from ?.

This simple initial condition is similar to that of ?, and implies that the binary system as a whole is not equilibrated. Therefore, as the simulation begins, the two WDs react to the tides, become stretched, and strong Roche lobe overflow ensues because the donor overshoots its Roche radius (in a widely separated binary, the donor would start to pulsate). As a result, the donor disrupts after just one to two orbits. For synchronized binaries, ? showed that the onset of mass transfer is much more gentle if the WDs are relaxed in the binary potential, disruption occurring only after several dozen orbital periods. They also showed that this results in systematic changes in the merger remnants. It is not clear whether the same will hold for unsynchronized binaries, since the accretion stream hits a surface that, in its frame, counterrotates, and therefore accretion is always much less gentle than for synchronized WDs. The difference is particularly dramatic for similar-mass binaries, where, in the synchronized case, the WDs can come into gentle contact, while in the unsynchronized case, any contact is violent. Unfortunately, it is difficult to test the effect of proper equilibration for unsynchronized binaries, since one has to relax to non-trivial initial conditions. A better approximation was attempted by ? and ?, who started their WDs further out and reduced the separation artificially until mass transfer began. In their simulations, disruption still followed very quickly. Given that, and wanting to avoid any partial synchronization, we kept our simpler setup, and tested it by running simulations with varying  $a_0$ . We will discuss these tests in Sec. ?? and compare our results with those of others in Sec. ??.

### 2.2.3 Merger Completion Time

It is difficult to decide when a merger is “complete”, since for some cases remnant properties continue to evolve long after the two WDs coalesce, with (artificial) viscosity redistributing angular momentum and heating the remnant. As a visually inspired criterion, we decided initially to use the degree of non-axisymmetry, continuing simulations until they were less than 2.5% non-axisymmetric, as measured from the ratio of zeroth to largest non-zero Fourier coefficient of particles binned in azimuth. However, this had its own issues: in dissimilar-mass mergers – where most of the particles are in the accretor, already roughly axisymmetric following the merger – our convergence criterion was achieved while the outer disk was still obviously non-axisymmetric. In equal-mass mergers, which are inherently more axisymmetric, completion also was too soon, before the densest material had reached the center of the remnant.

For the majority of our systems, however, the time required to reach 2.5% non-axisymmetry was roughly constant in units of the initial orbital period, at  $6.1 \pm 1.2$ . For about the same time, axisymmetry was also achieved (by subjective visual inspection) for both dissimilar-mass mergers (except, in extreme dissimilar-mass cases, the outermost regions of their disks) and for equal-mass mergers (where the densest material had reached the center). We therefore use 6 orbital periods of the initial binary as the completion time of our simulations. In Sec. ??, we discuss the effect of continuing our simulations for 2

further orbital periods.

## 2.3 Results

With our 48 simulated mergers in hand, we try to determine scaling relations of global quantities such as the remnant and disk mass, highest temperature, etc., and look for homologies in the remnant profiles. For our analysis, we use a cylindrical  $(\omega, \phi, z)$  coordinate system centered on the remnant core. Properties on the equatorial  $(\omega, \phi)$  plane – defined as the original orbital plane – are averaged over  $\phi$  using particles within  $\frac{1}{2}h_z$  of the equatorial plane, where  $h_z$  is the remnant’s rotational axis ( $\omega = 0$ ) central scaleheight (see Sec. ??). Properties along the rotational ( $z$ ) axis are averaged within a cylinder  $\omega < \frac{1}{2}h_z$ . We use  $\frac{1}{10}h_z$  as the bin size along both the equatorial plane and rotational axis. We determine properties mostly as a function of enclosed mass  $M(r)$ , which we define spherically<sup>3</sup>. Thus, we show, e.g., equatorial plane temperature  $T(\omega)$  as a function of  $M(r = \omega)$ , the mass enclosed within a sphere with radius  $r = \omega$ .

### 2.3.1 Representative Mergers

As found for previous simulations, qualitatively the most important factor controlling the merger outcome is whether the WD masses are “dissimilar” or “similar”. In the former case, where the donor is significantly less massive than the accretor, only the donor overflows its Roche lobe,<sup>4</sup> is disrupted, and accretes onto the accretor. The accreted material is heated on impact, lifting degeneracy. Hence, the merger remnant consists of a partly non-degenerate hot envelope and small, thick sub-Keplerian disk, both surrounding a cold core containing the largely unaffected accretor.

In the latter case of a similar-mass merger, there is a large degree of mixing between the two stars. For exactly equal masses, both stars are disrupted simultaneously, and their accretion streams impact each other near the system’s barycenter. Material from the centers of both stars initially forms a thick, cold, dense torus orbiting the barycenter; this torus slowly shrinks due to viscous drag, pushing the accretion stream material above and below the equatorial plane. When the stars have slightly different mass, the lower-mass one disrupts first, forming an accretion stream (or series of streams) that mixes with accretor material down to the center of the accretor (regardless of whether or not the other also disrupts).

We show the differences between similar and dissimilar-mass merger remnants using two representative examples in Figs. 2.1 and 2.2: a  $0.4 - 0.8 M_{\odot}$  highly dissimilar and a  $0.6 - 0.6 M_{\odot}$  equal-mass merger, respectively. One sees that the remnant morphologies are very different, consistent with previous work. The  $0.4 - 0.8 M_{\odot}$  merger features a cold, nearly non-rotating and thus spherically symmetric remnant core, surrounded by a hot envelope with roughly equal degeneracy and thermal support, which itself is surrounded on the equatorial plane by a rotationally supported non-degenerate thick disk that holds most of the angular momentum. The accretor forms the core, largely undisturbed by the merger, while the envelope and disk are composed almost entirely out of donor material. The hottest points are on the interface between the core and the envelope.<sup>5</sup> The  $0.6 - 0.6 M_{\odot}$  remnant, on

---

<sup>3</sup>Arguably, enclosed mass is more properly defined within equipotential surfaces, but this makes comparison with other simulations harder. For dissimilar-mass mergers, the difference is slight.

<sup>4</sup>The lower mass WD is larger and thus always fills its (smaller) Roche lobe first.

<sup>5</sup>The higher temperatures near the core are spurious; see Sec. ??

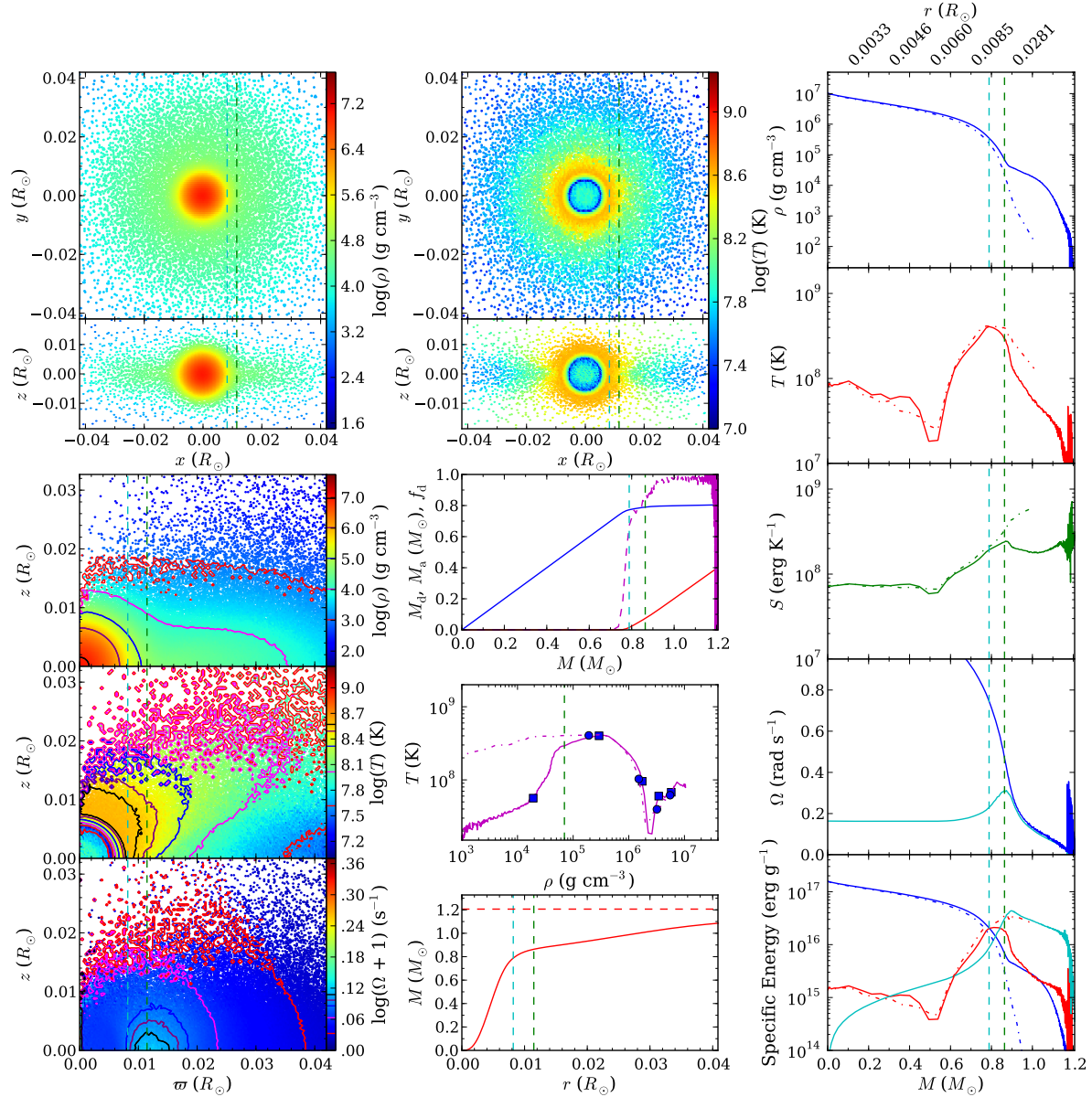


Figure 2.1: Structure of a  $0.4 - 0.8 M_{\odot}$  merger remnant, representing the general outcome of a merger of white dwarfs with dissimilar mass. Upper left and middle – binned maps of density  $\rho$  and temperature  $T$  along slices in the  $xy$  and  $xz$ -planes. Lower left – binned maps and contours of density, temperature, and angular frequency  $\Omega$  in the  $(\omega, z)$  plane, averaged over cylindrical coordinate  $\phi$  and over  $\pm z$  (with 1 added to  $\Omega$  to avoid problems with the logarithmic intensity scale). Middle – enclosed masses of donor and accretor material  $M_{\mathrm{d}}$  and  $M_{\mathrm{a}}$  (solid red and blue, resp.), and fraction of donor material  $f_{\mathrm{d}}$  at a particular mass shell (dashed magenta). Middle, one but lowest – temperature-density profile with enclosed masses in  $0.2 M_{\odot}$  increments indicated, both along the equatorial plane (solid curve, squares) and along the rotational axis (dot-dashed curve, circles). Middle, bottom – enclosed mass as a function of  $r$ , with the total mass indicated by the horizontal dashed red line. Right-hand column, top to bottom - density, temperature, entropy, angular (cyan) and Keplerian (blue) frequency, and degeneracy (blue), thermal (red) and rotational (cyan) specific energies as a function of enclosed mass  $M$ , both along the equatorial plane and along the rotational axis (solid and dot-dashed curves, respectively). In all graphs, the start of the disk (where the centrifugal acceleration equals half the gravitational one) and the equatorial radius (or mass enclosed within) of maximum temperature are marked by vertical green and blue dashed lines, respectively. [See the electronic edition of the Journal for Figs. 1.1–1.48.]

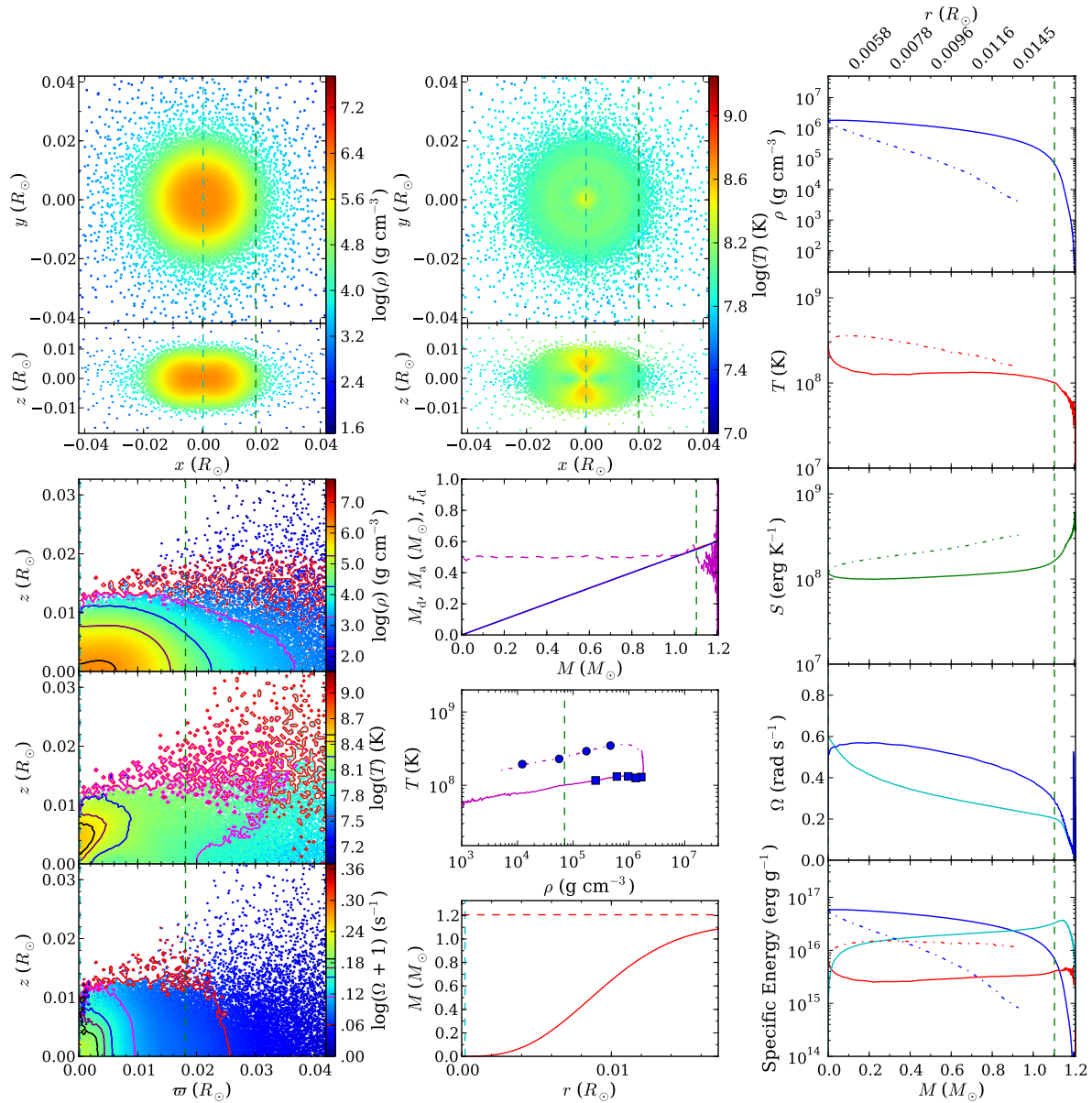


Figure 2.2: As Fig. Set 2.1, but for a  $0.6 - 0.6 M_\odot$  merger remnant, representing the general outcome of a similar-mass merger.

the other hand, has a massive, hot, partly rotationally supported and thus ellipsoidal core, and a very small but thick disk, both of which consist of material from both stars. No distinct envelope is formed. The hottest points are within the remnant core, just above and below the equatorial plane, arising from accretion stream material pushed out by the shrinking dense torus.

A good way to visualize how mergers transition between dissimilar and similar-mass is to look at changes in the remnant properties with varying donor mass. In Fig. ??, we show curves for accretors of 0.65 (left) and  $1.0 M_{\odot}$  (right). One sees that remnants of highly dissimilar-mass mergers, with mass ratio  $q_m \equiv M_d / M_a \lesssim 0.5$ , have properties resembling the  $0.4 - 0.8 M_{\odot}$  merger: their donor and accretor barely mixed, their temperature curves have off-center hot plateaus, and their angular velocity profiles feature an off-center bump. The equal-mass,  $q_m = 1$  cases resemble the  $0.6 - 0.6 M_{\odot}$  remnant: they have flat temperature profiles and centrally peaked angular velocity profiles. Intermediate cases have intermediate profiles, with the bumps in the temperature and angular velocity profiles widening with increasing  $q_m$ . The  $0.4 - 0.8 M_{\odot}$  and  $0.6 - 0.6 M_{\odot}$  remnants therefore lie at the extremes of what merger remnants look like.

The similarity between some of the curves for the  $0.65$  and  $1.0 M_{\odot}$  accretors in Fig. ?? suggests a homology. The similarity is closest for mergers with the same mass difference  $\Delta M$ , as can be seen in Fig. ???. For equal-mass mergers, all profiles are similar, simply scaled by a factor that depends on the total mass (except the  $1.0 - 1.0 M_{\odot}$  merger; see below). As  $\Delta M$  increases, the profiles are slightly less similar: with increasing total binary mass, the degree of mixing decreases, and the temperature and angular velocity maxima drift to slightly lower fractional enclosed mass. Nevertheless, the profiles still resemble one another far more closely than they resemble curves with other  $\Delta M$ . The same holds for profiles along the rotational axis.

It may seem surprising that the controlling parameter between these approximate homologies is the mass difference  $\Delta M$  rather than the mass ratio  $q_m$ . Empirically, however, the case is clear: e.g., the  $0.4 - 0.5$  (second column, yellow) and  $0.8 - 1.0 M_{\odot}$  (third column, black) mergers have the same  $q_m$ , but different  $\Delta M$ , and their structures clearly differ from one another. The same is true for the  $0.4 - 0.6$  (third column, cyan) and  $0.6 - 0.9$  (fourth column, brown)  $M_{\odot}$  mergers. As we discuss below, the similarity of mergers of similar  $\Delta M$  likely reflects the close relation between the ratio of central densities and mass difference.

Before discussing the homologies and trends further, we should note the one dramatic exception. The  $1.0 - 1.0 M_{\odot}$  simulation differs fundamentally from its fellow  $\Delta M = 0$  mergers. During the evolution of this system, unlike for all other equal-mass mergers, one WD was fully disrupted before the other, and as a result material from one star (arbitrarily designated the “donor” before the start of simulation, hence the “inverted” mixing profile in Figs. ?? and ??) preferentially resides near the center of the remnant. This system also often appears as an outlier in Sec. ?? below. The  $0.9 - 0.9 M_{\odot}$  merger also did not have equal mixing between the two stars, though the difference is much smaller. ? noticed the same effect in their simulations, and concluded it reflected the fact that more massive WDs are much more concentrated and therefore harder to disrupt. This seems a likely explanation.

# Bibliography

- Abbott, B. P., Abbott, R., Abbott, T. D., et al. 2016, Physical Review Letters, 116, 131102
- Andronov, N., Pinsonneault, M. H., & Terndrup, D. M. 2006, ApJ, 646, 1160
- Justham, S., Podsiadlowski, P., & Vink, J. S. 2014, ApJ, 796, 121
- Kaiser, N., Burgett, W., Chambers, K., et al. 2010, in Proc. SPIE, Vol. 7733, Ground-based and Airborne Telescopes III, 77330E
- Knigge, C., Leigh, N., & Sills, A. 2009, Nature, 457, 288
- LSST Science Collaboration, Abell, P. A., Allison, J., et al. 2009, ArXiv e-prints, arXiv:0912.0201
- Nandez, J. L. A., Ivanova, N., & Lombardi, Jr., J. C. 2014, ApJ, 786, 39
- Rau, A., Kulkarni, S. R., Law, N. M., et al. 2009, PASP, 121, 1334
- Rosswog, S. 2015, International Journal of Modern Physics D, 24, 1530012
- Tylenda, R., Hajduk, M., Kamiński, T., et al. 2011, A&A, 528, A114
- van Kerkwijk, M. H., Chang, P., & Justham, S. 2010, ApJ, 722, L157
- Yungelson, L. R. 2005, in American Institute of Physics Conference Series, Vol. 797, Interacting Binaries: Accretion, Evolution, and Outcomes, ed. L. Burderi, L. A. Antonelli, F. D'Antona, T. di Salvo, G. L. Israel, L. Piersanti, A. Tornambè, & O. Straniero, 1–10